

A mathematical model of the immune system's role in obesity-related chronic inflammation

Toby Shearman

May 7, 2009

Abstract

Obesity is quickly becoming a pandemic. The low-grade chronic inflammation associated with obesity leads to health risks such as cancer, heart disease, and type 2 diabetes mellitus. To better understand the progression of obesity-related chronic inflammation, mice were fed either a high fat or low fat diet over 140 days. At days 0, 35, 70, and 140, the percentages of macrophage subsets, CD4+ T cells, and regulatory-T cells infiltrating the intra-abdominal white adipose tissue (WAT) were examined. Monocyte chemoattractant protein-1 (MCP-1) mRNA expression in WAT was also quantified. Additionally, glucose-normalizing ability was examined by administering peritoneal glucose tolerance tests. This research was conducted during a ten-week research experience for undergraduates. A group of eight undergraduate students participated: Pablo Díaz, Michael Gillespie, Justin Krueger, José Pérez, Alex Radebaugh, Toby Shearman, Garret Vo, and Christine Wheatley. I continued this research independently during the Fall 2008 semester. The REU site was sponsored by NSF and hosted at the Interdisciplinary Center for Applied Mathematics and Virginia Bioinformatics Institute at Virginia Tech.

A system of ordinary differential equations models this system. The model consists of 8 differential equations, has 25 parameters, and has 1 forcing function. While I played an integral role in the development of the model as a whole, my major individual contribution was characterizing the model. Tools I used to characterize the model include parameter estimation, see *Sections 2.3* and *2.4*, and sensitivity analysis, see *Section 3.1*. Based on the data provided, the system describes the growth of adipocyte size and chronic inflammation over 105 days beginning at day 35, which is approximately when the adipose cells become hypertrophic. The model shows that without intervention, chronic inflammation escalates and the related health problems persist.

1 Introduction

Obesity, which is defined as a body mass index over 30, continues to grow as a health concern in the United States. As recently as July 2008, the Centers for Disease Control reported a phone survey that shows approximately 26 percent of Americans over the age of 18 are obese [4]. Other research shows that the prevalence of obesity has increased by 70 percent over the past decade [9]. According to World Health Organization estimates, over 300 million adults are obese [11]. As the severity of the problem continues to grow worldwide, many scientific experts consider the obesity crisis a pandemic [10].

Low-grade chronic inflammation is currently believed to be the most probable link between obesity and its comorbidities. Unlike acute inflammation, which is the natural response to injury or infection, chronic inflammation results from a defective immune response. The excessive activity of pro-inflammatory cells and proteins can result in additional defects for surrounding tissues.

These effects of chronic inflammation can lead to diseases such as cancer, kidney failure, atherosclerosis, and type 2 diabetes mellitus.

When a body is obese, the adipocyte cells swell to abnormal volumes (hypertrophy). As the adipocytes continue to enlarge, the cells' endoplasmic reticulum comes under excessive stress and fails. This leads to the excessive production of pro-inflammatory proteins such as monocyte chemoattractant protein-1 (MCP-1) and tumor necrosis factor- α (TNF- α) [2]. MCP-1 is a chemokine that attracts cells expressing the C-C motif chemokine receptor 2 (CCR2) on their cell surface [12]. This is relevant because recent studies have shown that the migration of macrophages expressing the glycoprotein F4/80 and CCR2 at high concentrations is associated with impaired glucose tolerance [5].

The release of TNF- α and MCP-1 and the subsequent progression of chronic inflammation are shown in Figure 1 below.

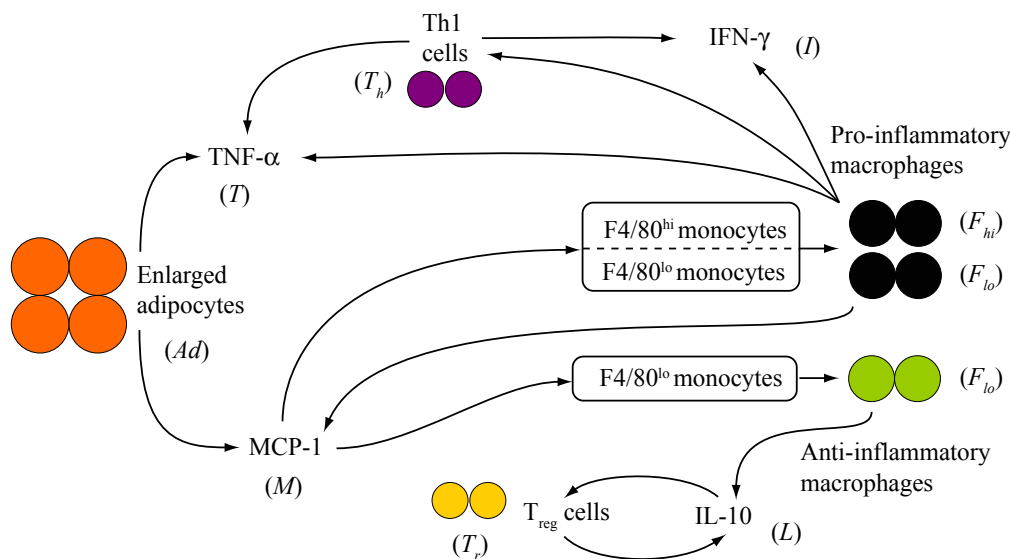


Figure 1: Diagram of Chronic Inflammation.

The monocytes that reach the white adipose tissue interact with various cytokines to differentiate into 4 characterized subsets of macrophages. The four subsets are M1, M2, deactivated, and transforming growth factor- β (TGF- β). M1 and deactivated macrophages are the most relevant subsets to the system. M1 macrophages are induced by the presence of interferon- γ (IFN- γ) and secrete interleukin-12 (IL-12), MCP-1, and TNF- α . Deactivated macrophages are induced by IL-10 and also secrete IL-10 [13].

T cells are also drawn to the adipose tissue. Many of the T cells are already differentiated into pro-inflammatory

and anti-inflammatory cells once they reach the adipose tissue, but a significant portion of the differentiation is due to the same cytokines that convert monocytes to macrophages. The interaction between naïve T cells and interleukin-12 (IL-12) produces pro-inflammatory T helper (Th1) cells. The Th1 cells produce IFN- γ , more MCP-1, and more TNF- α , which further contribute to the inflammation. Similarly, the interaction between naïve T cells and interleukin-10 (IL-10) produce anti-inflammatory T regulatory (T_{reg}) cells. The T_{reg} cells manufacture and release more IL-10 [1].

This research aims to aid and complement current stud-

ies on chronic inflammation by building a mathematical model that accurately reflects the interactions of the macrophages, T cells, chemokines, and cytokines that cause chronic inflammation. The model provides quantitative insight into the progression of chronic inflammation that would not otherwise be possible due to the limits of data collection.

2 Model/Methods

2.1 Experiment and Data

Drs. Josep Bassaganya-Riera and Amir Guri performed all the experiments and collected all the data used for this research in their lab at the the Virginia Bioinformatics Institute at Virginia Tech.

A collection of C57BL/6J mice were separated into three test groups: high-fat diet, low-fat diet, and control. The mice were put in identical environments that prevented any opportunities for exercise, so there would be no variations other than their diet. At day 0 the control group was sacrificed and necropsied; on days 35, 70, and 140 of the experiment mice on high-fat and low-fat diets were also sacrificed and necropsied.

The percentage of macrophage subsets, CD4+ T cells, and regulatory T cells in the white adipose tissue (WAT) were collected using flow cytometry. MCP-1 and TNF- α gene expression in the WAT were measured using real-

time RT-PCR. Finally, glucose-normalizing ability was examined using a peritoneal glucose tolerance test.

The amount of available data varies depending on what species is being viewed. Averages are taken for the four time points for the mice on the high fat diet. In addition, the day 35 data is interpolated for Th1, T_{reg} and MCP-1 because data does not exist. Initially, we have a total of four average data points for MCP-1, T cells and macrophages; however, the scope of our model decreases the data to three reference points, days 35, 70 and 140.

Having the cell data as a percentage of the total cells in the stromal-vascular fraction (SVF) poses a problem because the data reflects any changes in the rest of the SVF, which the model cannot possibly do. Our model assumes the change in the number of stromal-vascular cells not considered in the model to be zero and converts between the data given as percentages and cell counts to solve the system, which presents an additional assumption.

2.2 System of Equations

The model has nine variables and twenty-five parameters. The system consists of eight differential equations, six of which are linear. A ninth equation characterizes the forcing function. Some agents that contribute to obesity-induced inflammation are not accounted for. In our system we only considered the following factors:

Table 1: List of abbreviations and the corresponding system factor.

Abbreviation	Corresponding Factor
Ad	Adipocyte Size
T	TNF- α
M	MCP-1
F_{hi}	F4/80 ^{hi} CCR2 ⁺ macrophages
F_{lo}	F4/80 ^{lo} CCR2 ⁺ macrophages
T_h	T helper 1 cells
I	IFN- γ
T_r	T _{reg} cells
L	IL-10

We consider day 35, the approximate time for average adipocyte hypertrophy, as the beginning of our model. Adipocytes secrete TNF- α and MCP-1. TNF- α is a cytokine that increases insulin resistance, and MCP-1 plays a significant role in the recruitment of monocytes expressing CCR2 on their surface. The monocytes that MCP-1 recruits to the site are classified as high or low, corresponding to the expression of F4/80 on the cell surface. The F4/80^{hi} monocytes (F_{hi}) only become pro-inflammatory macrophages and the F4/80^{lo} monocytes (F_{lo}) are uncharacterized, producing either pro or

anti-inflammatory macrophages [2]. Pro-inflammatory macrophages contribute to the production of IFN- γ , a cytokine that is also secreted by Th1 cells. Anti-inflammatory macrophages secrete IL-10, which is also released by T_{reg} cells. From this overview, the system of equations seen below is created. In the system, cells are measured as populations, and protein concentrations are measured in gene expressions (pg-cDNA/ μ g-RNA). The adipocyte size is measured by the cross-sectional area (μ m²) of the adipocytes.

$$\frac{dT(t)}{dt} = k_1(F_{hi}(t) + \alpha F_{lo}(t)) + k_2Ad(t) + k_3T_h(t) - d_1T(t) \quad (1)$$

$$\frac{dM(t)}{dt} = k_4(F_{hi}(t) + \alpha F_{lo}(t)) + k_5Ad(t) - d_2M(t) \quad (2)$$

$$\frac{dF_{hi}(t)}{dt} = k_6 \left(M(t)I(t) - \frac{\alpha M(t)L(t)}{1 - \alpha} \right) - d_3F_{hi}(t) \quad (3)$$

$$\frac{dF_{lo}(t)}{dt} = k_7M(t)L(t) + k_8 \frac{\alpha M(t)L(t)}{1 - \alpha} - d_4F_{lo}(t) \quad (4)$$

$$\frac{dT_h(t)}{dt} = k_9(F_{hi}(t) + \alpha F_{lo}(t)) + m_1 - d_5T_h(t) \quad (5)$$

$$\frac{dI(t)}{dt} = k_{10}T_h(t) + k_{11}(F_{hi}(t) + \alpha F_{lo}(t)) - d_6I(t) \quad (6)$$

$$\frac{dT_r(t)}{dt} = k_{12}L(t) + m_2 - d_7T_r(t) \quad (7)$$

$$\frac{dL(t)}{dt} = k_{13}T_r(t) + (1 - \alpha)k_{14}F_{lo}(t) - d_8L(t) \quad (8)$$

$$Ad(t) = a\sqrt{t} + b \quad (9)$$

We consider all of the F4/80^{hi} macrophages to be pro-inflammatory. However, the F4/80^{lo} macrophages are uncharacterized, so we define α to be the fraction of F4/80^{lo} macrophages that are pro-inflammatory.

MCP-1 attracts monocytes with CCR2 receptors; therefore, we assume that given a nonzero concentration of MCP-1 there are monocytes available in the adipose tissue. For the purpose of this model, the representative interaction between MCP-1 and IFN- γ differentiates the monocytes into pro-inflammatory macrophages, and the representative interaction between MCP-1 and IL-10 differentiates the monocytes into anti-inflammatory macrophages.

Equation (1) represents the rate of change in the concentration of TNF- α with respect to time. TNF- α is initially released by the enlarged adipocytes in the system, although the main production of this cytokine is accredited to pro-inflammatory macrophages [2]. The term $(F_{hi}(t) + \alpha F_{lo}(t))$ describes the total number of pro-inflammatory macrophages. Th1 cells also produce TNF- α . The concentration of TNF- α decreases due to its denaturation.

Equation (2) represents the change in concentration of MCP-1 with respect to time. MCP-1 is also initially released by the enlarged adipocytes in the system. Once monocytes become M1 macrophages, however, the activated macrophages, presumably F4/80^{hi}CCR2+ macrophages, contribute to MCP-1 concentrations [5].

The change in the population of F4/80^{hi} macrophages with respect to time is represented by Equation (3). The first term accounts for the production of all F4/80^{hi} macrophages while the second term determines the number of pro-inflammatory macrophages that are F4/80^{lo}. The third term accounts for their death.

The change in the population of F4/80^{lo} is represented in Equation (4). The first term accounts for the interaction of F4/80^{lo} monocytes with IL-10 to produce anti-inflammatory F4/80^{lo} macrophages. The second term, like in Equation (3), represents the F4/80^{lo} monocytes that become pro-inflammatory macrophages. The third term accounts for macrophage death.

In Equation (5), the pro-inflammatory macrophages release interleukin 12 (IL-12), which differentiates naïve T cells into Th1 cells. The presence of pro-inflammatory macrophages, $(F_{hi}(t) + \alpha F_{lo}(t))$ implies the presence of IL-12 since pro-inflammatory macrophages produce IL-12. For simplicity, we take advantage of this relationship and assume that the Th1 cell population is dependent on pro-inflammatory macrophages. The term m_1 accounts for any migration of Th1 cells to the site, naturally occurring or by chemokines and cytokines we are not considering in our model. Finally, $d_5T_h(t)$ represents the removal or death of Th1 helper cells.

Th1 cells and pro-inflammatory macrophages produce IFN- γ , so they directly increase the concentration of IFN- γ . The IFN- γ concentration decreases with its de-

naturation or internalization by its receptor, which is shown in Equation (6).

In regard to Equation (7), IL-10 increases the concentration of adaptive T regulatory cells by differentiating naïve T cells. The term m_2 accounts for any migration of T regulatory cells to the site. Finally, $d_7 T_r(t)$ represents the death of T regulatory cells.

T regulatory cells and anti-inflammatory macrophages secrete IL-10 during the immune response. The concentration decreases through denaturation or internalization by its receptor, as shown in Equation (8).

Adipocyte size (Ad) has a logarithmic correlation with body weight, for which we have data [3]. Equation (9) represents the enlargement of adipocytes with respect to time.

2.3 Parameter Estimation with Matlab™

Our model includes 25 parameters. Fourteen of these parameters describe interaction rates, eight describe component degradation, two describe cell migration rates, and one (α) defines the fraction of F4/80^{lo} macrophages that are pro-inflammatory. Several of the parameters may be amenable to special laboratory observations; many other parameters only make sense within the context of the mathematical model (1-9). Because experimental procedures isolating each effect are impractical, we are led to mathematical methods to characterize good parameter values.

To evaluate the quality of a parameter set, we quantitatively describe the error of the corresponding solution against available data using the 2-norm – the distance between the solution and the data. Due to concerns about the MCP-1 data, the calculation ignores the MCP-1 data. The following cost function is evaluated using the percentage of total cells for F4/80^{hi} and F4/80^{lo} macrophages, Th1 cells, and T regulatory cells at days 35, 70, and 140. The equation for the error $J(p)$ is below:

$$J(p) = \frac{1}{2} \sum_k \|x(t_k; p) - \hat{x}(t_k)\|^2.$$

Table 2: Final Values for the 8 Initial Conditions, x_0

State	Value*	State	Value*
T	2.74×10^{-5}	M	1.12×10^{-5}
F_{hi}	1.176×10^1	F_{lo}	1.331×10^1
T_h	1.679×10^1	I	3.4×10^{-5}
T_r	2.968×10^0	L	7.270×10^{-5}

*Cell values are cell populations (in thousands) and protein values are measured in pg-cDNA/ μ g-RNA.

Defining an appropriate range for each parameter is important for implementing a random search method for which we write an algorithm. As the model is written, all parameters are defined to be positive. Unfortunately, we have no further knowledge of the interaction parameters ranges; therefore, these were selected in the range [0, 0.1] in order to maintain reasonable cell populations. The values for k_6 , k_7 , and k_8 are set equal due to their similar nature. Based on equilibrium constraints of equations (5) and (7), functions of d_5 and d_7 , respectively, determine m_1 and m_2 parameters. Once inside the adipose tissue, macrophages survive on the order of months, so the ranges for the degradation of F4/80^{hi} and F4/80^{lo} macrophages are [0, 1]. We expect the proteins and other immune cells to live on the order of hours and days, respectively, and their initial ranges are set accordingly. Finally, we set α equal to zero since the latest experimental data shows a very high percentage, if not all, of the F4/80^{lo} macrophages are anti-inflammatory.

In order to solve the system of eight coupled-differential equations, we implemented one of MATLAB’s built-in ODE solver—`ode15s`. This differential equation solver was used because non-stiff equation solvers, like the Runge-Kutta 4-5 algorithm (`ode45`), were incapable of solving our system.

Three optimization methods were used to decrease the error and so to better match the system solution and the data: a random search method, a Nelder-Meade unconstrained minimization procedure (`fminsearch`), and a constrained-nonlinear minimization algorithm (`fmincon`). `Fminsearch` is part of the standard Matlab software suite, whereas `fmincon` is part of the Optimization Toolbox.

The initial conditions are experimental values from day 35. After selecting a parameter set which minimizes the error and adheres to the constraints, we allow the initial conditions to vary, along with all 25 parameters. Adjusting the initial conditions improves the overall-fit. We select the following set of initial conditions and parameters to characterize our model:

Table 3: Final Values for the Parameter Set, p

Parameter	Value	Parameter	Value
k_1	7.10×10^{-9}	k_8	1.71×10^{10}
k_2	4.22×10^{-8}	k_9	6.82×10^{-7}
k_3	5.81×10^{-8}	k_{10}	7.66×10^{-6}
k_4	5.70×10^{-14}	k_{11}	1.16×10^{-5}
k_5	6.88×10^{-9}	k_{12}	1.60×10^4
k_6	1.42×10^{10}	k_{13}	1.04×10^{-4}
k_7	1.07×10^{10}	k_{14}	9.11×10^{-6}
d_1	6.289	d_5	1.472
d_2	2.474	d_6	7.700
d_3	0.569	d_7	0.628
d_4	0.842	d_8	5.798
m_1	23.44	m_2	0.586
α	0.0		
a^\dagger	3.421×10^2	b^\dagger	2.046×10^3

[†]These parameters are characterized in [3]

Note that the largely different values of the collected data (cell counts and gene expressions), as discussed before, produce a staggering range for the parameter set. Parameter values associated with the interactions of MCP-1 with other proteins (which both have experimental values on the order of 10^{-5}) will have parameter values on the order 10^{10} . Likewise, parameter values associated with the production of proteins by cells will have values on the order of 10^{-10} or often smaller because a large number of cells is producing relatively small concentrations of proteins. Scaling the units of the parameters may improve the aesthetics, but likely would not change the results.

2.4 Further Parameter Estimation in COPASI™

During the Fall 2008 semester, COPASI became the home of this model. COPASI, or Complex Pathway Simulator, is a well-established software application used for simulating, analyzing, and characterizing biochemical networks [7]. COPASI is developed for systems like the proposed model. Particle swarm, simulated annealing, genetic, and other sophisticated algorithms are available within this software. Further parameter estimation was performed using the algorithms available in COPASI.

We implemented particle swarm with varying initial parameter sets. The results from the summer research experience were used as an initial set; however, most initial sets were randomly generated. Utilizing a simple perl script, we seeded hundreds of runs. Note that even thousands of different initializations of the particle swarm method are dwarfed within a 25-dimensional pa-

parameter space and even within a 16-dimensional space, which is achieved by understanding the underlying biology.

Our final approach to parameter estimation was simulated annealing. Simulated annealing is a robust, and often times consuming, global optimization technique. Inspired by statistical mechanics and solidification of crystals, Kirkpatrick *et al.* first introduced the inherent connection between these two seemingly isolated concepts [8].

Our efforts with COPASI provided parameter sets equivalent to the final parameter set found during the summer research using less sophisticated techniques. This result supports an unfortunate conclusion. Provided the large number of unidentified parameters and the limited data set, sophisticated techniques should be more successful at locating good parameter sets. This suggests underlying issues with the model. Further research into the critical interactions of the biological system is required. Our model is likely over-simplifying the system and overlooking a critical interaction or species.

3 Results

After deciding upon a specific set of parameters, we numerically solve the system of equations. Each subsequent solution is graphed independently as seen below. The solution is obtained using one of MATLAB's™ built-in ODE solvers. Several plots show the average data points to which the solution is fitted, while the remaining solutions are a product of the system.

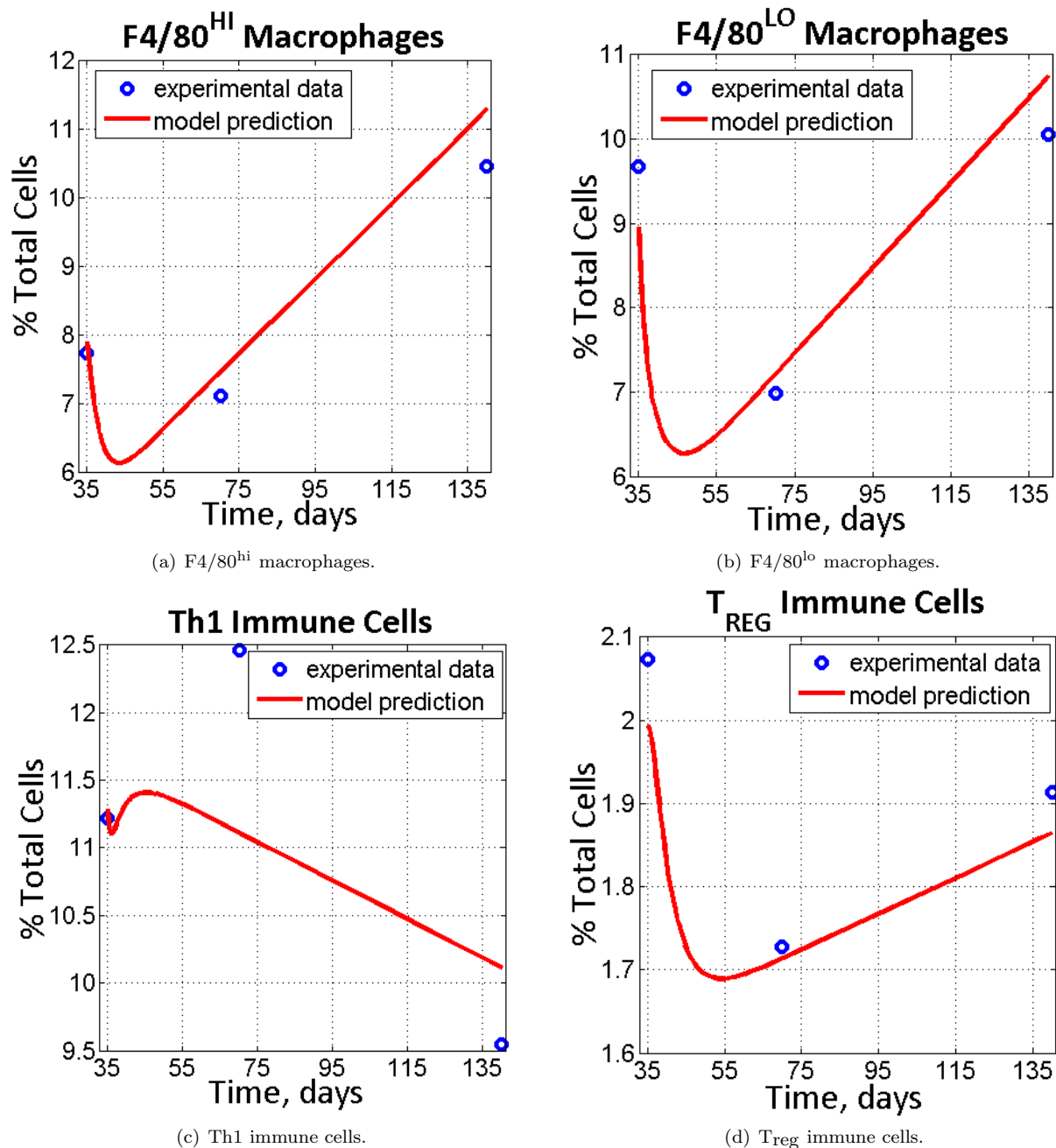
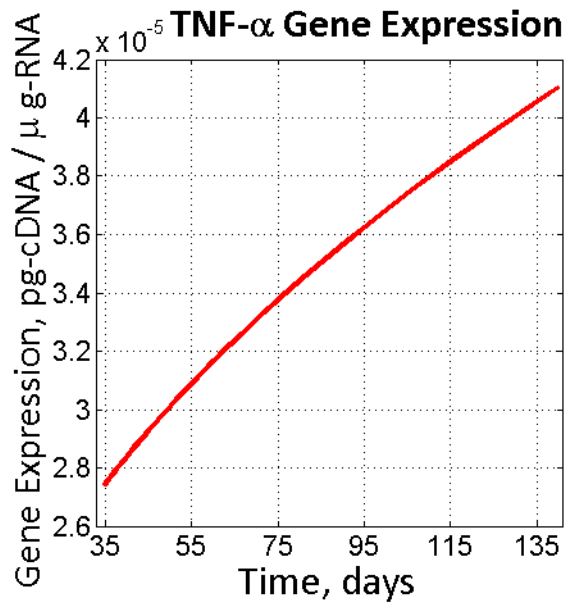


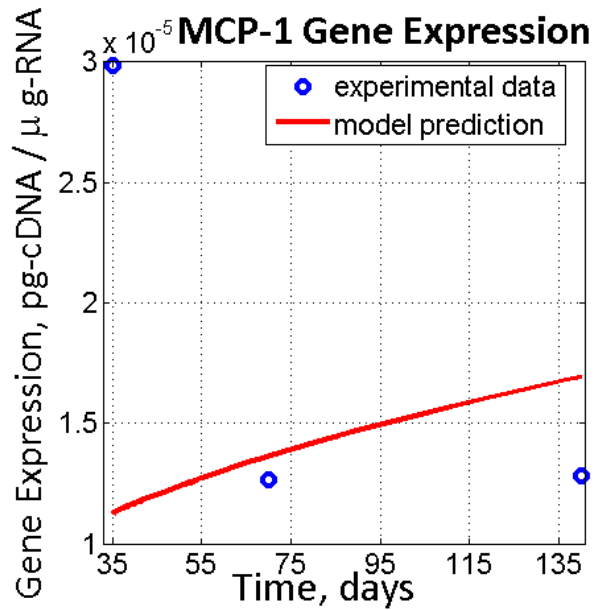
Figure 2: Collection of results for cell populations in percentages: (a) F4/80^{hi}, (b) F4/80^{lo}, (c) Th1, and (d) Treg

The percentage of F4/80^{lo} macrophages out of total cells is shown to follow the same general trend as the F4/80^{hi} macrophages, steeply decreasing followed by a significant increase in the last 95 days (Figure 2(b)). The percentage of F4/80^{lo} macrophages at day 140 is slightly smaller than the percentage of F4/80^{hi} macrophages at the same time. The error is also relatively small between the solution and plotted data points.

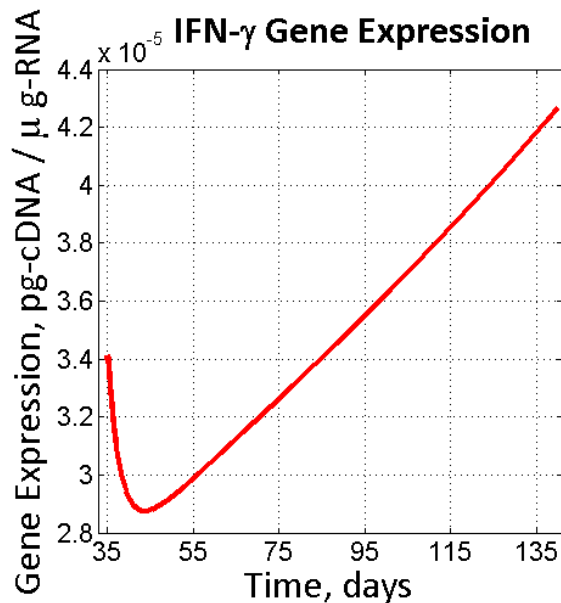
The percentage of Th1 cells decreases slightly, possibly due to the rapid decline of the cell population to equilibrium. This is followed by a quick increase and finally a steady decline for the 105 day period, which is shown in Figure 2(c). The overall decline is a result of the increase in the total number of other cells in the system. The interesting behavior associated with the percentage of Th1 will be discussed in more detail.



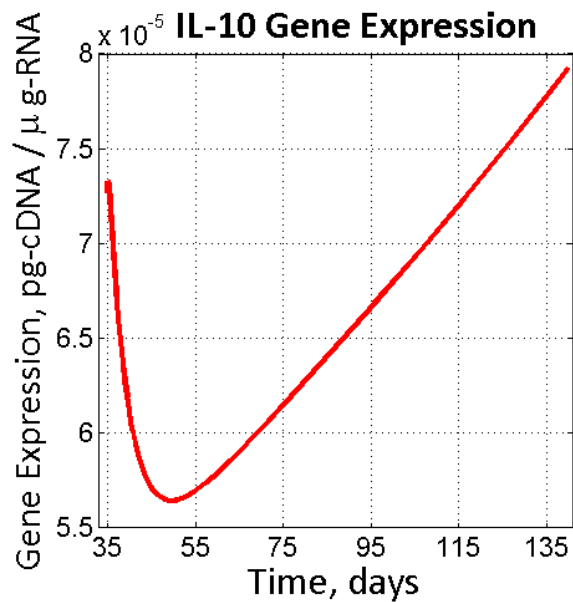
(a) TNF- α gene expression.



(b) MCP-1 gene expression.



(c) IFN- γ gene expression.



(d) IL-10 gene expression.

Figure 3: Collection of results for gene expressions: (a) TNF- α , (b) MCP-1, (c) IFN- γ , and (d) IL-10

From day 35 to day 140, the gene expression for MCP-1 gradually increases (Figure 3(b)). It is important to note that while the average data points for MCP-1 are plotted, the solution is found independently from the data.

3.1 Sensitivity Analysis

Understanding how the solution changes with respect to the parameters' changes can give insight into the biology. Therefore, analyzing how sensitive the model is with respect to the parameters becomes important. We

describe the sensitivities mathematically by

$$S_i^j = \frac{\partial x_i}{\partial p_j},$$

where i represents a particular state variable (1-8), and j signifies the particular parameter (1-25). The matrix $[S_i^j]$ consists of 200 entries, and is time-dependent.

We compute the sensitivities of our non-linear system by solving the coupled state/sensitivity initial value problem. Define $\bar{S}^j(t)$ by summing the sensitivities over each of the i (state) values, $\bar{S}^j(t) = \sum_{i=1}^8 |S_i^j|$. $\bar{S}^j(t)$ pro-

vides insight into how each parameter affects the system as a whole, at a given time, t . As seen Figure 4, sensitivity analysis helps identify important parameters like k_5 , d_2 , and d_8 . Figure 4 depicts the system's sensitivities to

each parameter, summed over the eight states and integrated from day 35 to 140. In terms of $\bar{S}^j(t)$, Figure 4 shows $\int_{35}^{140} \bar{S}^j(t) dt$ for each of the j (parameter) values.

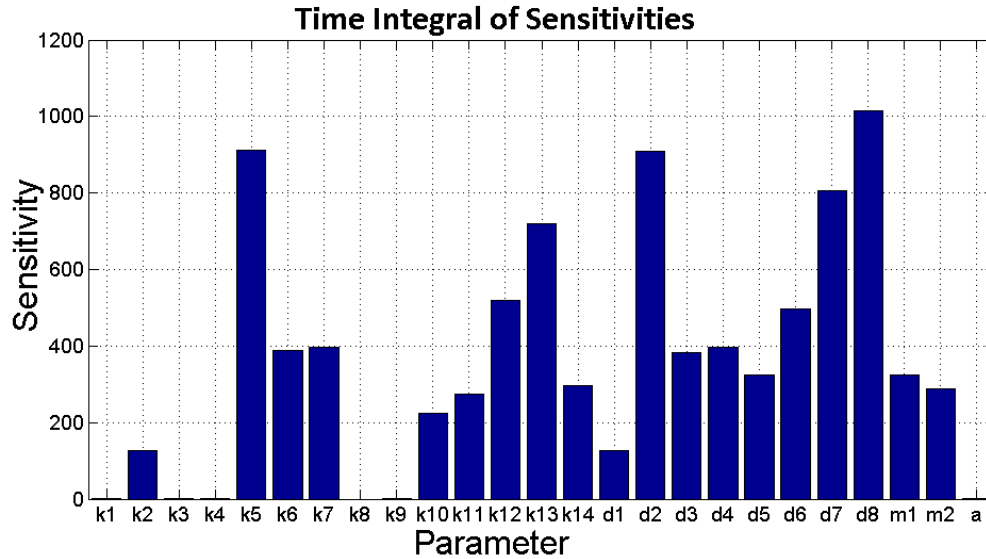


Figure 4: Sensitivities with respect to each of the 25 parameters—summed over the state-space, and integrated with respect to time.

Each of the sensitivities has been scaled by both their respective parameter value and the average value of the state over days 35 to 140 to understand the relative sensitivities. Moreover, it is important to recognize that these are local values. The sensitivities depend on the area of existence in the parameter and time spaces; with different parameter sets and at different times the sensitivities may change drastically.

Considering figures like Figure 5 and Figure 6, which reveal more information than 4, provides a more complete understanding of the system. Figure 5 shows an example of three parameters, k_{12} , k_{13} , and k_{14} , which emphasize that parameter sensitivities are local values with respect to time.

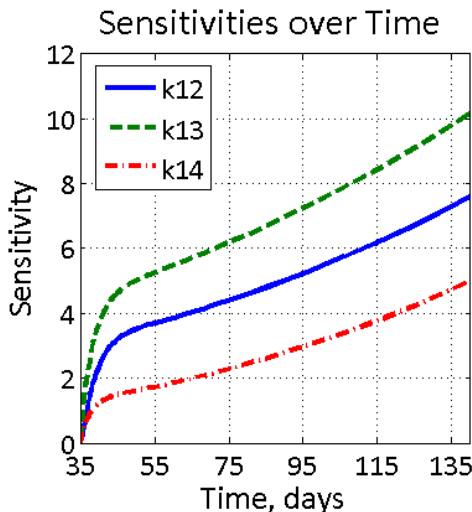


Figure 5: Sensitivities of the system to k_{12} , k_{13} , and k_{14} summed over the state-space, emphasizing the change

To further understand the impact and importance of these sensitivities in the parameter estimation process, consider the gradient of the cost function:

$$J(p) = \frac{1}{2} \sum_k \|x(t_k; p) - \hat{x}(t_k)\|^2$$

in which k represents the time steps where data was gathered, and \hat{x} denotes the experimental data set. Differentiating with respect to the parameters gives:

$$\frac{\partial J(p)}{\partial p_j} = \sum_k \left[\|x(t_k; p) - \hat{x}(t_k)\| \cdot \frac{\partial x(t_k)}{\partial p_j} \right].$$

The gradient of the cost function contains $\frac{\partial x_i}{\partial p_j}$, which are the sensitivities. For non-zero error terms, $[x(t_k; p) - \hat{x}(t_k)]$ in the equation, the corresponding sensitivities drive that error's contribution to the gradient. Hence, highly sensitive parameters control large changes in the cost function. The gradient and an understanding of the sensitivities will help in implementing a more sophisticated parameter optimization technique.

Time-Integrated Sensitivities of States

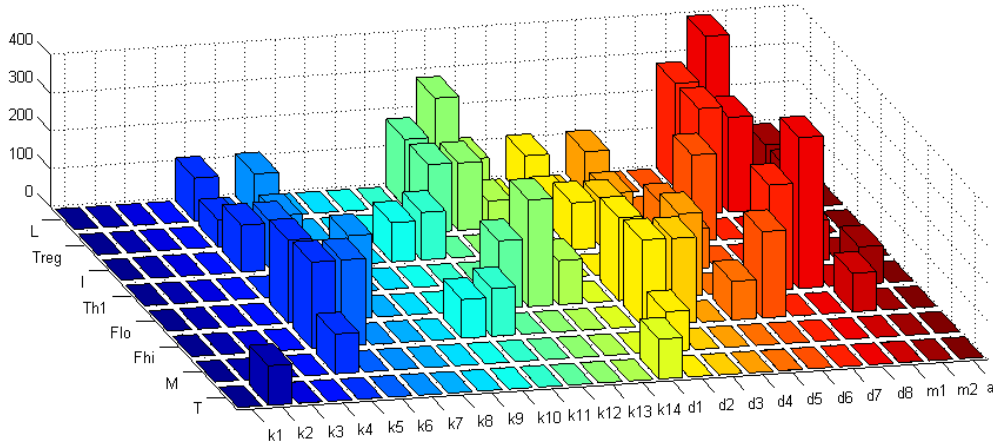


Figure 6: Sensitivities of each of the 8 variables with respect to each of the 25 parameters, integrated with respect to time.

4 Discussion

F4/80^{hi} macrophages and F4/80^{lo} macrophages are the prime area of interest and drive the system. As seen in Figures 2(a) and 2(b), F4/80^{hi} and F4/80^{lo} macrophages, respectively, more accurately fit the data when compared to the other six variable solutions. The solution for the percentage of F4/80^{lo} macrophages is similar in shape to the solution for percent F4/80^{hi} macrophages. However, F4/80^{lo} increases at a slower rate, which can be seen more easily when the model extends beyond 140 days. As inflammation worsens, it is expected for pro-inflammatory macrophages to be greater in number than anti-inflammatory macrophages. The solution shows a greater percentage of F4/80^{hi} macrophages than F4/80^{lo} macrophages at day 140, which can be viewed as a faster production rate in the inflamed area.

Th1 cell count exhibits interesting behavior. Figure 7, below, shows this unique behavior of Th1 cells in the system. Regardless of the initial condition, the Th1 cell count stabilizes quickly to a constant population. Since the Th1 cell population remains constant, the percentage of Th1 will vary according to the rest of the system. As the macrophages decrease, the Th1 percentage naturally increases and finally when the macrophage percentage increases, the Th1 percentage will decrease. The nature of the Th1 cells needs to be further explored as it is surprising to see a constant cell count indicating the possibility of a missing component in Equation 5.

Limitations exist and assumptions must be identified when observing the model. The first issue lies in the data used to select the parameters and to judge the validity of the model. As discussed in the Model and Methods section, the sparsity of data as well as the units of the data both add complications to the model.

Th1 Cell Count - Initial Condition Scan

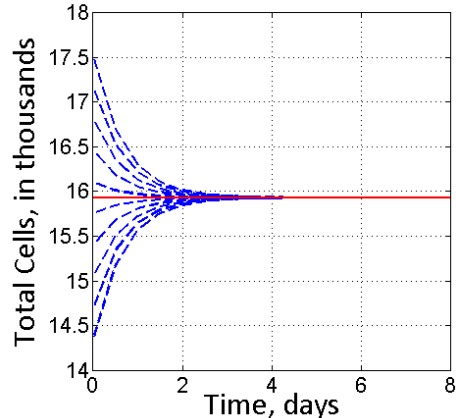


Figure 7: Th1 cell population with varying initial conditions.

The design of the model reflects the interactions of the macrophages, T cells, chemokines, and cytokines that cause chronic inflammation, after the onset of adipocyte hypertrophy. The model does not account for the time period in which the subject becomes obese. Using body weight data for our study of interest by Guri et al, we track average adipocyte sizes over a period of 140 days, and note day 35 as being a threshold for problematic adipocyte hypertrophy [6]. Hence the day 0 data was not used in our model. In addition, the MCP-1 data acquired was questionable due to the sporadic nature of the results. When finding parameters, we are only confident in using the F4/80^{hi}, F4/80^{lo}, Th1 and T_{reg} data for our base platform. This constitutes an over-parameterized problem decreasing the confidence in our initial conditions and model and leaving ample room for improvement in the future when more data is available.

The extensive parameter estimation work, as previously

discussed, highlights an underlying issue of the proposed model. Sophisticated parameter estimation algorithms, like those implemented in this research, with 25 degrees of freedom, should be able to recreate the limited data set. This suggests that we have overlooked a critical interaction or have incorporated an interaction we do not fully understand.

The model must be confined within some set of biological boundaries. The immune system encompasses many systems in the body along with various other proteins and cell types ignored in this model in attempts to simplify a complex problem. Immune cells, such as monocytes, travel throughout the body via blood and lymph, but our model isolates the specific destination of these immune cells, the white adipose tissue due to the well established significance of intra-abdominal fat inflammation. The F4/80 macrophages, T_{reg} , Th1 cells and specific corresponding proteins, IL-10, IFN- γ , TNF- α , and MCP-1 are extracted from the SVF as focal points for our model. All other components of the SVF are assumed to remain constant in our model.

Ultimately a model should reasonably project into the future, but this model is designed for the small 105 day experimental period of adipocyte hypertrophy. As seen by Figure 8, expanding the time span causes the model to fail.

At about 535 days, the F4/80^{hi} macrophages count grows to nearly 1 million cells for every initial twelve thousand macrophages. We must adjust the system of equations in order to apply the model past Day 140.

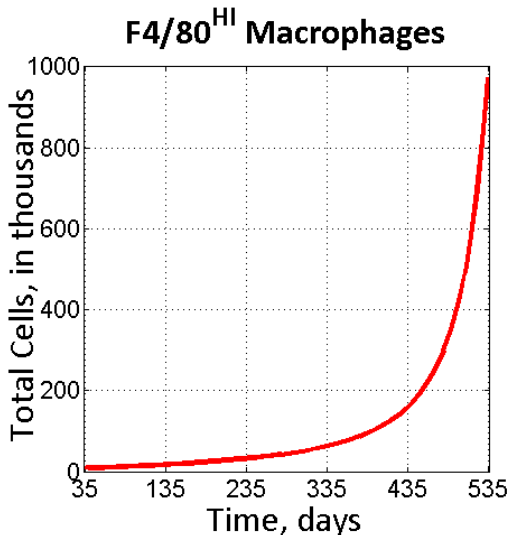


Figure 8: F4/80^{hi} macrophage population.

5 Conclusion and Future Work

With obesity continuing to grow as a pandemic, national governments such as the United States have established

initiatives to reduce the number of obese citizens over a certain time frame [4]. This makes an understanding obesity-related inflammation both timely and urgently needed.

We have developed a mathematical model to quantify the molecular and cellular interactions of chronic inflammation. We fit the solution for the model to the experimental data. The F4/80^{hi} macrophages increase at a steep rate. The F4/80^{lo} macrophages and T regulatory cells also increase but at a lesser rate than the F4/80^{hi} macrophages. The chemokine and cytokine levels all also increase which is expected due to the increase in the numbers of cells that produce these proteins. The solution also presents two major discrepancies from the expected results: the percentage of Th1 cells decreases, and in looking at the cell count, the Th1 population rapidly decreases to an equilibrium where it resides for the remainder of the time. The other unexpected result is the initial decrease in the percentages and cell populations for both macrophage types and both T cell types.

The limitations and assumptions of the model allow for improvements and further work on the continuous model. The model's simulation capabilities start at day 35, approximately when adipocyte hypertrophy sets in. Extending the model to include day 0 information will improve the biological relevance of the model. Understanding how the adipose cells reach hypertrophy and the immune system's response in the first 35 days is just as important as understanding what occurs in the adipose tissue after the adipocytes reach hypertrophy.

Similarly, extending the model to accurately reflect the progression of chronic inflammation beyond 140 days would improve the model's value. While the current model has the capability of simulating beyond 140 days, the accuracy of the results are questionable since there is no data for extended time spans currently available to validate the model. The ability to project the changes in chronic inflammation over an experimental subject's lifespan makes the model easier to apply for future research. In addition, having a model that is valid over extended periods of time reduces the necessity of experimental research to gain valuable insight into a biological system.

A highlight of future work is adding the effect of drug treatments to the model, which also promises to give a better and more relevant system of equations. Similarly, finding a way to incorporate the relationship between inflammation and insulin resistance would be extremely beneficial. If the model could accurately reflect drug treatments' role in chronic inflammation, a better understanding of how chronic inflammation progresses could result. The drug treatment model could also lead to new ideas for research both in the function of the

immune system and in the drugs used to treat chronic inflammation. The research that could stem from the system of equations modeling capabilities could lead to newer, more effective drugs that treat chronic inflammation with fewer side-effects.

Our model and the corresponding solution have positive results. The solution reflects what is known to occur as chronic inflammation progresses. The solution does, however, present some questions about the validity of the system. The discrepancies with the biology

could result from the limitations of the data, numerical error, or the absence of key components in the system of equations. Even with the inconsistencies, our model can improve by incorporating more data, more significant variables, or even by simply modifying the equations to better imitate the biological interactions. While the model is currently unrefined, it has the potential to grow and develop into a future work benefiting research on obesity, chronic inflammation and type 2 diabetes mellitus.

6 Acknowledgements

The authors are grateful for support provided by the National Science Foundation and the National Institutes of Health under grants:

- NSF Award #0755322 REU Site: Modeling and simulation of biological networks
- NIH/NSF Award #0609225 Summer Institute for Quantitative and Integrative Bioengineering
- NCCAM at NIH Award # 5R01AT4308

Additional support was provided by the Nutritional Immunology Group at the Virginia Bioinformatics Institute, the Virginia Bioinformatics Institute, and the Interdisciplinary Center for Applied Mathematics at Virginia Tech. We would also like to thank Drs. Josep Bassaganya-Riera and Amir Guri for providing the data and biological insight necessary to perform the research. We would like to thank Christy Koelling and Drs. Jeff Borggaard, John Burns, Eugene Cliff, Raquel Hontecillas-Magarzo, Abdul Jarrah, Reinhard Laubenbacher, Henning Mortveit, and Lizette Zietsman for their contributions to discussions and oversight of the research. In addition, we would like to thank The MathWorksTM for providing software through their academic support program.

References

- [1] J. BASSAGANYA-RIERA, *Introduction to immunology lecture*. June 2008.
- [2] ———, *Obesity-related inflammation lecture*. June 2008.
- [3] P. DÍAZ AND J. PÉREZ, *Average adipocyte area and its relationship to body weight in db/db high-fat-diet obese mice*. July 2008.
- [4] D. GALUSKA, C. GILLESPIE, S. KUESTER, A. MOKDAD, M. COGSWELL, AND C. PHILIP, *State-specific prevalence of obesity among adults—united states, 2007*, Morbidity and Mortality Weekly Report, 57 (2008), pp. 765–768.
- [5] A. GURI, R. HONTECILLAS, G. FERRER, O. CASAGRAN, U. WANKHADE, A. NOBLE, D. EIZIRIK, F. ORTIS, M. CNOP, D. LIU, H. SI, AND J. BASSAGANYA-RIERA, *Loss of PPAR γ in immune cells impairs the ability of abscisic acid to improve insulin sensitivity by suppressing monocyte chemoattractant protein-1 expression and macrophage infiltration into white adipose tissue*, Journal of Nutritional Biochemistry, 19 (2008), pp. 216–228.
- [6] A. GURI, R. HONTECILLAS, H. SI, D. LIU, AND J. BASSAGANYA-RIERA, *Dietary abscisic acid ameliorates glucose tolerance and obesity-related inflammation in db/db mice fed high-fat diets*, Clinical Nutrition, 26 (2007), pp. 107–116.
- [7] S. HOOPS, S. SAHLE, R. GAUGES, C. LEE, J. PAHLE, N. SIMUS, M. SINGHAL, L. XU, P. MENDES, AND U. KUMMER, *Copasi—a complex pathway simulator*, Bioinformatics, 22.
- [8] S. KIRKPATRICK, C. GELATT, AND M. P. VECCHI, *Optimization by simulated annealing*, Science, 220 (1983), pp. 671–681.
- [9] A. MOKDAD, B. BOWMAN, E. FORD, F. VINICOR, J. MARKS, AND J. KOPLAN, *The continuing epidemics of obesity and diabetes in the united states*, Journal of the American Medical Association, 286 (2001), pp. 1195–1200.

- [10] B. POPKIN AND C. DOAK, *The obesity epidemic is a worldwide phenomenon*, Nutrition Review, 56 (1998), pp. 106–114.
- [11] P. PUSKA, C. NISHIDA, AND D. PORTER, *World health organization strategy on diet, physical activity, and health: Obesity and overweight*. Data and statistics. WHO, 2007.
- [12] S. SHOELSON, J. LEE, AND A. GOLDFINE, *Inflammation and insulin resistance*, Journal of Clinical Investigation, 116 (2006), pp. 1793–1801.
- [13] S. YONA AND S. GORDON, *Inflammation: Glucocorticoids turn the monocyte switch*, Immunology and Cell Biology, 85 (2007), pp. 81–82.